

Photopumped green lasing on BeZnSeTe double heterostructures grown on InP substrates

Ichirou Nomura,^{a)} Katsumi Kishino, Tomoya Ebisawa, Yutaka Sawafuji, Rieko Ujihara, Kunihiro Tasai, Hitoshi Nakamura, Tsunenori Asatsuma, and Hiroshi Nakajima
Department of Engineering and Applied Sciences, Sophia University, 7-1 Kioi-cho, Chiyoda-ku, Tokyo 102-8554, Japan

(Received 10 September 2008; accepted 7 December 2008; published online 13 January 2009)

Double heterostructures (DHs) consisting of BeZnSeTe active and MgSe/BeZnTe superlattice cladding layers were fabricated on InP substrates by molecular beam epitaxy. By photoexciting the DHs, green lasing emissions at 548 nm were obtained at room temperature. The threshold excitation power density was 70 kW/cm², from which we estimated the threshold carrier density and threshold current density assuming a green laser diode (LD) with a BeZnSeTe active layer to be $(1.4\text{--}4.6) \times 10^{18}$ cm⁻³ and 0.22–0.73 kA/cm², respectively. The experiment proved the applicability of BeZnSeTe as an active layer of green LDs. © 2009 American Institute of Physics. [DOI: 10.1063/1.3058761]

The green laser diode (LD) is one of the crucial research topics remaining in the optical device field. Green LDs are very attractive for laser light sources of the three primary colors, high luminance laser pointers, and so on. II-VI compound semiconductors are one of the promising materials for realizing green LDs.

Blue-green ZnCdSe/MgZnSSe II-VI LDs on GaAs substrates were extensively studied in the 1990s. Room-temperature (RT) continuous wave operations were reported in 1993.^{1,2} However, the study and developments were interrupted because the device lifetime could not be extended beyond 400 h.³ The investigation of the degradation mechanism causing the short lifetime of the LDs clarified that the degradation could be ascribed to pre-existing microscopic point defects, such as N-related deep donors in the MgZnSSe *p*-cladding layer,^{4,5} their diffusion induced by compressive crystal strain in the ZnCdSe active layers,^{6,7} and electron leakage into the *p*-cladding layer.⁸ The short lifetime as a result of such defect generation and diffusion is originally brought about by the weakness in the crystal bonds of the ZnSe-based II-VI crystals.

On the other hand, we have pointed out different II-VI compounds such as MgZnCdSe, BeZnTe, and BeZnSeTe grown on InP substrates.^{9–13} Especially, BeZnSeTe (Ref. 11) having direct bandgap energies from 2.1 (590 nm) to 2.7 eV (460 nm) is a promising active layer material for highly reliable yellow-to-green LDs and light emitting diodes (LEDs). The inclusion of beryllium chalcogenide components (i.e., BeSe and BeTe) into BeZnSeTe contributes to the strengthening of the lattice bonds owing to their high cohesive energy,¹⁴ which is effective for preventing defect diffusion, thereby lengthening the device lifetime. In addition, since the BeZnSeTe active layer is lattice-matched to the substrates, the compressive strain effect, which is responsible for enhancing the defect diffusion in the conventional ZnSe-based devices, is eliminated. In fact, we fabricated LEDs having the BeZnSeTe active layer and achieved yellow-to-green emissions and long lifetime operations of more than 5000 h.^{15,16}

In this study, we investigated the photopumped lasing characteristics of BeZnSeTe double heterostructures (DHs) grown on InP substrates to evaluate the applicability of BeZnSeTe as the active layer material of green LDs. In the experiment, green lasing emissions of around 548 nm were obtained at RT.

BeZnSeTe DHs were fabricated on S-doped (100) InP substrates by employing double-chamber molecular beam epitaxy (MBE). A cross-sectional schematic diagram of the DH is shown in Fig. 1. The DH was composed of a 100-nm-thick Be_{0.13}Zn_{0.87}Se_{0.38}Te_{0.62} active layer sandwiched by 0.2 μm (upper) and 1.2 μm (lower) MgSe/Be_{0.48}Zn_{0.52}Te (4 ML/4 ML) superlattice (SL) cladding layers,¹⁷ and 300 nm Zn_{0.48}Cd_{0.52}Se buffer and 3 nm ZnTe cap layers. After the growth of InP and InGaAs buffer layers on InP substrates in the III-V chamber, the II-VI layers were grown in the II-VI chamber along the following procedure; i.e., Zn flux irradiation onto the InGaAs buffer surface at 240 °C, ZnCdSe low-temperature buffer growth at 240 °C, ZnCdSe buffer growth at 280 °C, and other (cladding, active, and cap) layer growths at 300 °C. Each layer except for the ZnTe cap layer was grown under the lattice-matching conditions with the InP substrate. The ZnTe cap layer was introduced to avoid oxidation of the MgSe/BeZnTe SL upper cladding layer. Although the cap layer has a large lattice-mismatching (3.9%)

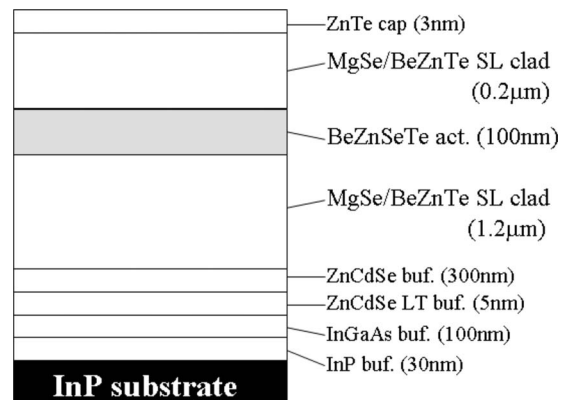


FIG. 1. Schematic cross section of BeZnSeTe DH.

^{a)}Electronic mail: ichirou@katsumi.ee.sophia.ac.jp.

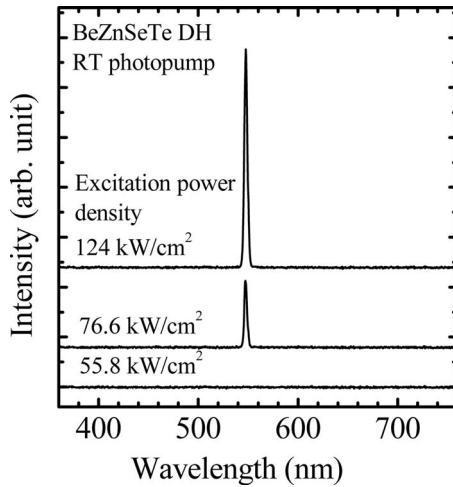


FIG. 2. Lasing spectra at excitation power densities of 55.8, 76.6, and 124 kW/cm².

and high absorption coefficient, the influence to the crystal quality and lasing properties was very low because the layer thickness was very thin (3 nm).

The grown wafer was cleaved into rectangular (about 5 × (1–2) mm²) shape for the photopumping measurement. The sample was excited under frequency-tripled Nd:YAG (YAG denotes yttrium aluminum garnet) laser light (355 nm) irradiation at RT. The pulse width was 5 ns and the repetition rate was 20 Hz. The laser light was focused, using a cylindrical lens, onto the sample surface to form a stripe geometry excitation region. The emission spectra of the light radiated from the cleaved facet were detected with a multichannel spectrum analyzer. Typical emission spectra at excitation power densities of 55.8, 76.6, and 124 kW/cm² for the 1.85-mm-cavity-length sample are shown in Fig. 2. Above the excitation power density of 76.6 kW/cm², the green lasing emissions at 548 nm were observed. The lasing light was polarized in the transverse electric mode. The peak intensity of the lasing spectrum was plotted as a function of the excitation power density, as shown in Fig. 3. The peak intensity rapidly increased above 70 kW/cm². From this, the threshold excitation power density P_{th} was estimated to be 70 kW/cm².

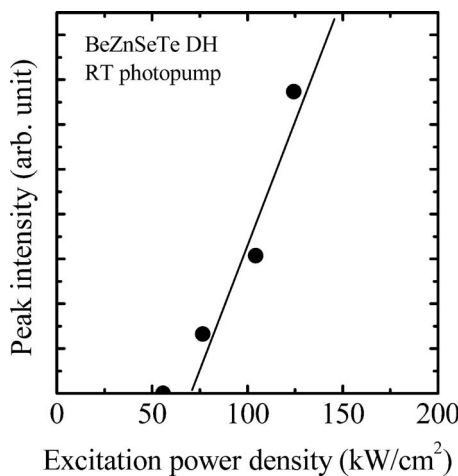


FIG. 3. Peak intensity of lasing spectrum as a function of excitation power density.

The threshold carrier density N_{th} can be calculated from the P_{th} value using

$$N_{th} = \frac{(1-R)P_{th}}{qE_p} \left\{ \frac{\tau_a}{t_a}(1 - e^{-\alpha_a t_a})e^{-\alpha_c t_{c1}} + \frac{\eta\tau_c}{t_{c1}}(1 - e^{-\alpha_c t_{c1}}) + \frac{\eta\tau_c}{t_{c2}}(1 - e^{-\alpha_c t_{c2}})e^{-\alpha_a t_a}e^{-\alpha_c t_{c1}} \right\} \quad (1)$$

and

$$R = (n_c - 1)^2 / (n_c + 1)^2, \quad (2)$$

where τ_a and τ_c are the carrier lifetimes in the active and cladding layers, respectively, q is the elementary electric charge, E_p is the photon energy of the excitation laser (355 nm), t_a , t_{c1} , and t_{c2} are the layer thicknesses of the active, upper cladding, and lower cladding layers, α_a and α_c are the absorption coefficients of the active and cladding layers, respectively, R is the reflectance at the sample surface (the top of the upper cladding layer), and n_c is the refractive index of the upper cladding layer.

In this estimation, it is assumed that the photoexcited carriers at the active layer and carriers injected into the active layer after excitation at the cladding layers contribute to lasing. Here, the carrier injection efficiency from the cladding into the active layer is denoted by η in Eq. (1). In the calculation, η is assumed to be several values from 0 to 1 because it is unknown. The internal quantum efficiency of the carrier excitation by photons is assumed to be 100%. We ignore the effects of the thin cap layer, the reflection, and the resonance at the interfaces between the active, cladding, and buffer layers. α_a , α_c , and n_c are 7.76×10^4 cm⁻¹, 6.18×10^4 cm⁻¹, and 3.43, respectively, which were experimentally estimated from the results of spectroscopic ellipsometry measurements of other BeZnSeTe and MgSe/BeZnTe SL samples. τ_a and τ_c are assumed to be 1 ns. Using the above parameters and Eqs. (1) and (2), the N_{th} values are estimated to be 1.4×10^{18} , 3.0×10^{18} , and 4.6×10^{18} cm⁻³, respectively, when $\eta=0$, 0.5, and 1.

In addition, in order to evaluate the lasing property and applicability of BeZnSeTe as an active layer of LDs, the threshold current density J_{th} assuming a LD structure with a BeZnSeTe active layer is estimated from the N_{th} values using

$$J_{th} = qN_{th}t_{lda}/\tau_a. \quad (3)$$

In this estimation, N_{th} of the LD is assumed to be equal to that of the DH. This assumption is valid if we can make the threshold gain of the LD equal to that of the DH, which is possible by adjusting the waveguide structure (i.e., the optical confinement factor), the cavity length, and the reflectance of the cavity mirror of the LD. In addition, the carrier injection efficiency into the active layer is assumed to be 100%, which means there is no radiative/nonradiative recombination component in any part except for the active layer and no leakage current from the active to the cladding layers. These factors are affected by the crystal quality, band discontinuities, and bandgap energy differences in each layer, and can be removed (or reduced at least) by optimizing the growth condition and material parameters. In Eq. (3), t_{lda} is the active layer thickness of the LD. t_{lda} and τ_a are assumed to be 10 nm and 1 ns, respectively. When $N_{th}=1.4 \times 10^{18}$ ($\eta=0$), 3.0×10^{18} (0.5), and 4.6×10^{18} cm⁻³ (1), J_{th} is estimated to be 0.22, 0.48, and 0.73 kA/cm², respectively. This shows

that J_{th} is at least less than 0.73 kA/cm^2 because η is less than 1. These values are comparable to those of J_{th} of commercialized AlGaInP red LDs and less than those of InGaN blue LDs ($J_{\text{th}} > 1 \text{ kA/cm}^2$), which indicates the high potential using BeZnSeTe as an active layer material of green LDs.

In conclusion, DHs consisting of a BeZnSeTe active and MgSe/BeZnTe SL cladding layers for photopumping lasing were fabricated on InP substrates by MBE. By photoexciting the samples, green lasing emissions at 548 nm were obtained at RT. The P_{th} was 70 kW/cm^2 . Using the P_{th} value, N_{th} and J_{th} assuming a LD with a BeZnSeTe active layer were estimated to be $(1.4\text{--}4.6) \times 10^{18} \text{ cm}^{-3}$ and $0.22\text{--}0.73 \text{ kA/cm}^2$, respectively. These results prove that BeZnSeTe is promising as an active layer of green LDs.

This work was partly supported by a Grant-in-Aid for Scientific Research (B) No. 19360166 and a Grant-in-Aid for Scientific Research on Priority Areas No. 18069010 from the Ministry of Education, Culture, Sports, Science and Technology of Japan.

¹N. Nakayama, S. Itoh, T. Ohata, K. Nakano, H. Okuyama, M. Ozawa, A. Ishibashi, M. Ikeda, and Y. Mori, *Electron. Lett.* **29**, 1488 (1993).

²A. Salokatve, H. Jeon, J. Ding, M. Hovinen, A. V. Nurmikko, D. C. Grillo, L. He, J. Han, Y. Fan, M. Ringle, R. L. Gunshor, G. C. Hua, and N.

Otsuka, *Electron. Lett.* **29**, 2192 (1993).

³E. Kato, H. Noguchi, M. Nagai, H. Okuyama, S. Kijima, and A. Ishibashi, *Electron. Lett.* **34**, 282 (1998).

⁴D. Albert, J. Nürnberger, V. Hock, M. Ehinger, W. Faschinger, and G. Landwehr, *Appl. Phys. Lett.* **74**, 1957 (1999).

⁵M. Adachi, Z. M. Aung, K. Minami, K. Koizumi, M. Watanabe, S. Kawamoto, T. Yamaguchi, H. Kasada, T. Abe, K. Ando, K. Nakano, A. Ishibashi, and S. Itoh, *J. Cryst. Growth* **214-215**, 1035 (2000).

⁶L.-L. Chao, G. S. Cargill III, T. Marshall, E. Snoeks, J. Petruzzello, and M. Pashley, *Appl. Phys. Lett.* **72**, 1754 (1998).

⁷A. Toda, K. Nakano, and A. Ishibashi, *Appl. Phys. Lett.* **73**, 1523 (1998).

⁸K. Katayama and T. Nakamura, *J. Appl. Phys.* **95**, 3576 (2004).

⁹T. Morita, A. Kikuchi, I. Nomura, and K. Kishino, *J. Electron. Mater.* **25**, 425 (1996).

¹⁰S.-B. Che, I. Nomura, W. Shinozaki, A. Kikuchi, K. Shimomura, and K. Kishino, *J. Cryst. Growth* **214-215**, 321 (2000).

¹¹Y. Takashima, I. Nomura, Y. Nakai, A. Kikuchi, and K. Kishino, *Phys. Status Solidi B* **241**, 747 (2004).

¹²K. Kishino and I. Nomura, *IEEE J. Sel. Top. Quantum Electron.* **8**, 773 (2002).

¹³K. Kishino and I. Nomura, *Phys. Status Solidi C* **1**, 1477 (2004).

¹⁴C. Vèrié, *J. Cryst. Growth* **184-185**, 1061 (1998).

¹⁵I. Nomura, Y. Nakai, K. Hayami, T. Saitoh, and K. Kishino, *Phys. Status Solidi B* **243**, 924 (2006).

¹⁶I. Nomura, T. Ebisawa, S. Kushida, K. Toyama, S. Kuroiwa, and K. Kishino, Abstract of International Symposium on Semiconductor Light Emitting Devices, ISSLED2008, Phoenix, 2008 (unpublished), Paper No. 6, p. 22.

¹⁷S.-B. Che, I. Nomura, A. Kikuchi, K. Shimomura, and K. Kishino, *Phys. Status Solidi B* **229**, 1001 (2002).